ALGEBRAIC GRID ADAPTATION METHOD USING NON-UNIFORM RATIONAL B-SPLINE SURFACE MODELING+

Jiann-Cherng Yang* and B. K. Soni**
NSF Engineering Research Center and
Department of Aerospace Engineering
Mississippi State University
Mississippi State, MS 39762

ABSTRACT

An algebraic adaptive grid system based on equidistribution law and utilized by the Non-Uniform Rational B-Spline (NURBS) surface for re-distribution is presented. A weight function, utilizing a properly weighted boolean sum of various flow field characteristics is developed. Computational examples are presented to demonstrate the success of this technique.

INTRODUCTION

Grid adaptive schemes are divided into two basic categories: differential and algebraic. The differential method is based on a variational approach where a function which contains a measure of grid smoothness, orthogonality, and volume variation is minimized by using a variational principle. This approach provides a solid mathematical basis for the adaptive method, but the Euler-Lagrange equations must be solved in addition to the original governing equations. On the other hand, the algebraic method requires much less computational effort, but the grid may not be smooth. The algebraic techniques are based on devising an algorithm where the grid movement is governing by estimates of the local error in the numerical solution. This is achieved by requiring the points in the large error regions to attract other points and points in the low error region to repel other points. One of the disadvantages of algebraic method is that it generates the unsmooth grid. The utilization of NURBS will generate the well-distributed smooth grid (Fig. 1).

An adaptive grid is a grid that controls the placement of grid points automatically based on the solution of the physical problem under consideration and allows optimal grid redistribution as the solution progresses. The accuracy of the numerical algorithm depends not only on the formal order of approximation but also on the distribution of grid points in the computational domain. The adaptive grid is one of the methods that can make the numerical algorithm more accurate. The grid adaptive scheme, presented in this paper, is based on the equidistribution principle.

+ Work partially funded by a research on a grant from Teledyne Brown Engineering Corp and AFOSR.

* Graduate Student, Aerospace Engineering, Student Member AIAA.

** Associate Professor, Aerospace Engineering, Mississippi State University, Sr. Member AIAA.

The development of the adaptive algorithm for the structured flow simulation is accomplished as a two step process. The first step is to define an adaptive weighting mesh (distribution mesh) (Ref. 1-2) on the basis of the equidistribution law applied to the flow field solution. The second, and probably the most crucial step, is to redistribute grid points in the computational domain according to the aforementioned weighting mesh. Adaptive weighting (distribution mesh) provides the information on the desired concentration of points to the grid redistribution scheme. The evaluation of weighting mesh is accomplished by utilizing the weight function representing the solution variation and the equidistribution law (Ref. 3). The selection of the weight function plays a key role in grid adaptation (Ref. 4-5). A new weight function utilizing a properly weighted boolean sum of various flowfield characteristics is defined. The redistribution scheme is developed by utilizing Non-Uniform Rational B-Spline Surface (NURBS) representation (Ref 6). The application of NURBS representation results in a well-distributed smooth grid by maintaing the fidelity of the geometry associated with boundary curves. Various computational examples are presented to demonstrate the success of these methods.

GRID ADAPTATION METHOD

The basis of the grid adaptation is the equidistribution law in one dimension (Ref. 8) applied to the flow field. The equidistribution law is represented as

$$x_\xi \, w = constant \qquad (1)$$

With the weight function w taken as a function of ξ, this is just the Euler equation for the minimization of the integral

$$I = \int_0^1 w(\xi)\, x_\xi^2 \, d\xi \qquad (2)$$

Applying the spring analogy form to the above integral, the point location x_i can be defined by (Ref. 8)

$$x_i = L \frac{\int_1^i \frac{d\xi}{w(\xi)}}{\int_1^N \frac{d\xi}{w(\xi)}} \quad (i=2, 3 \ldots\ldots, N-1) \qquad (3)$$

The integral in the denominator depends on the point distribution, amounting to a sum of $1/w$ over the points. However $\Delta\xi = 1$ by construction regardless of the distribution. Therefore, the integral in (3) is evaluated iteratively. The integral in the numerator is then also re-evaluated for each point, thus changing the point distribution again. This process must be continued until convergence before the final new distribution is obtained.

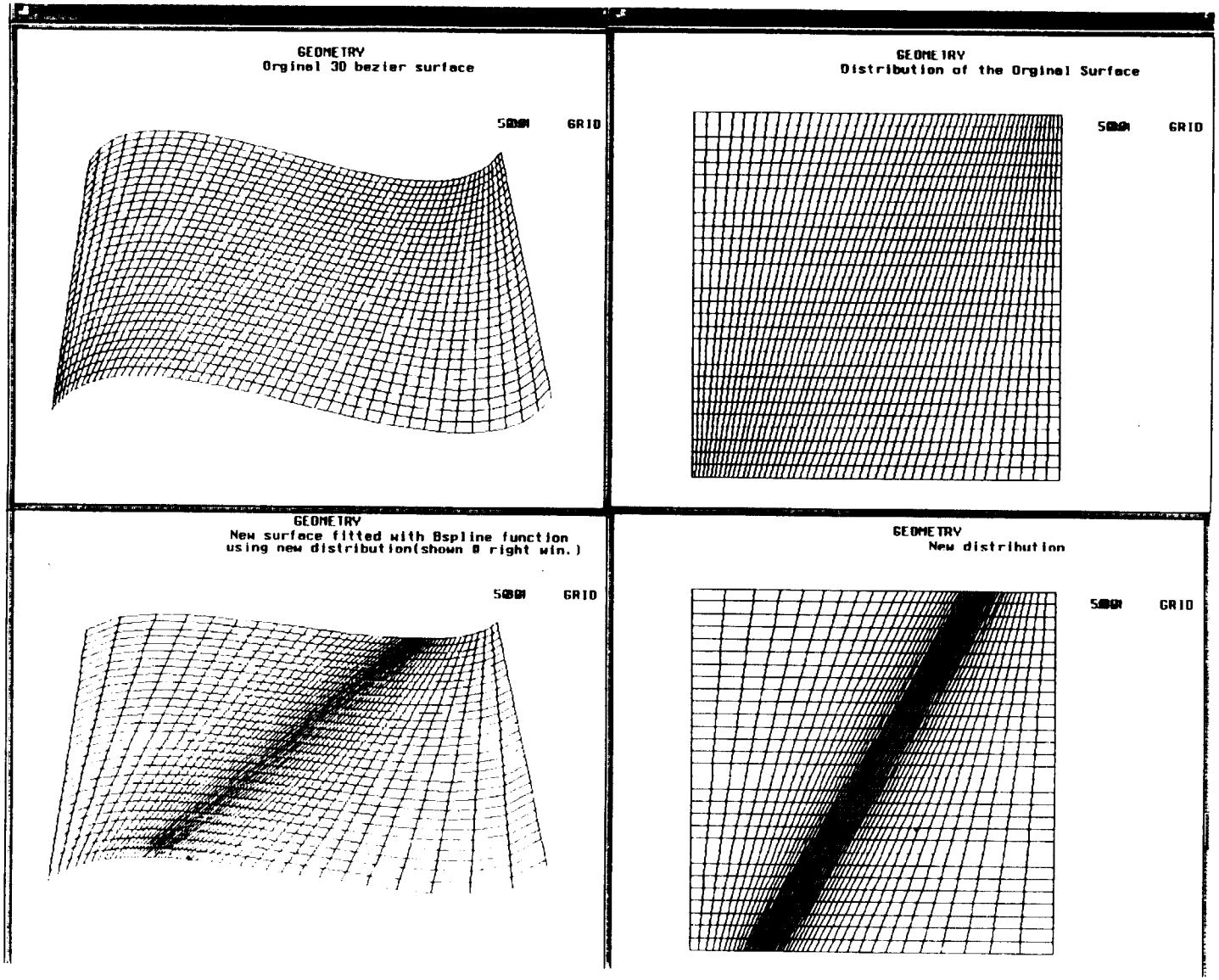

Physical domain

Computational domain

Figure 1.
Use NURBS surface to generate smooth grid.

ALGORITHM

A self-explanatory, pictorial view of the algorithm of algebraic adaptive grid generation is shown in Fig. 1.

The grid and solution will be transferred from the flow solver if the solution is good enough to apply grid adaptation. The criterion of good solution can be the pressure L^2 residue or another property of solution that can be used as the convergent indication.

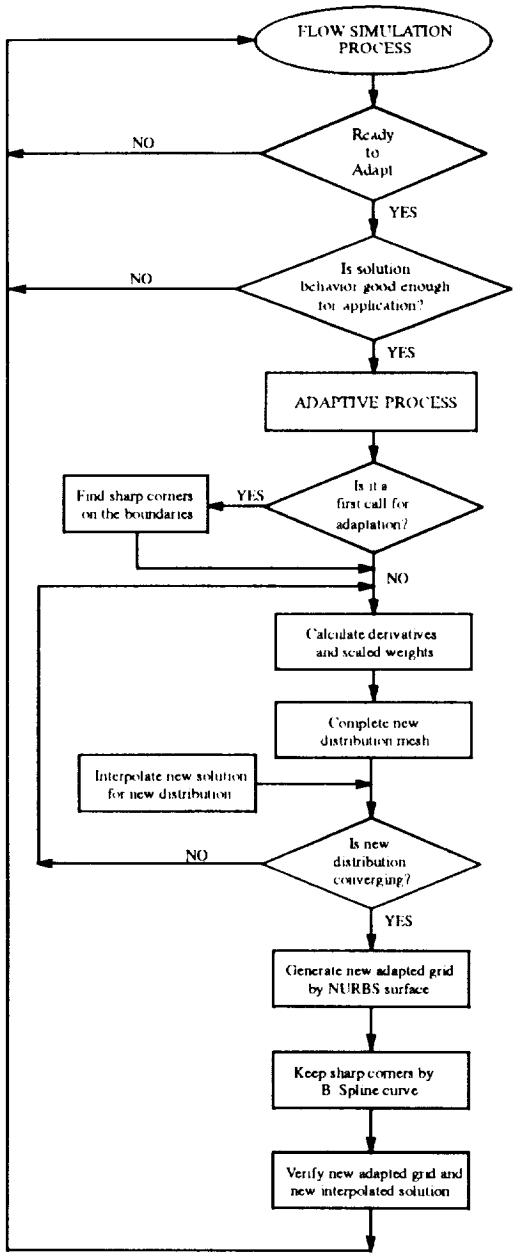

Figure 2.
Algorithm for 2−D Algebraic Adaptive Grid Generation System

WEIGHT FUNCTION

The weight function is a very important part in the adaptive grid system. Here we introduce a new weight function applicable to various flow field characteristics. The weight functions are computed in both the ξ and η computational directions, and then coupled adaptation is applied. A linear combination

$$1 + \sum_{j=1}^{N} \lambda_j w_j , \qquad with \sum \lambda_j = 1 \qquad (4)$$

where N – number of flow parameter (e.g. pressure, temperature, density, etc.)

λ_j – weighting factor associated with flow parameter $\lambda_j \geq 0$

$w_j - \alpha_j q_j \oplus \beta_j k_j = \alpha_j q_j + \beta_j k_j - (\alpha_j + \beta_j - 1) q_j k_j$

q_j – scaled gradient of the flow variable j such that $0 \leq q_j \leq 1$

k_j – scaled curvature values of the flow variable j such that $0 \leq k_j \leq 1$

$0 \leq \alpha_j \leq 1$, $0 \leq \beta_j \leq 1$, – weight factors assigned to gradients and curvatures is developed as the weight function utilizing the Boolean sum of contributions from scaled gradients and curvatures. The Boolean sum allows an appropriate weight to the gradients as well as the curvatures. For example, in the case of the j^{th} flow parameter, the influence of weights can be presented as follows:

q_j	k_j	α_j	β_j	w_j
1	0	1	β	1
1	0	α	β	α
0	1	α	1	1
0	1	α	β	β
1	1	1	1	1
1	1	α	1	1
1	1	1	β	1
1	1	α	β	1
0	0	α	β	0

Note that the value of the weight contribution is controlled by the weight factors and is at a maximum when gradients and/or curvature values are at a maximum. The gradients and curvatures associated with the flow characteristics under consideration are smoothed using a four point diffusion process.

SCALING SCHEME FOR α & β

Dwyer has developed a method to determine the percentage change in a dependent variable as a priori. (Ref. 9). This method is enhanced here to determine the suitable scaling α and β at each grid point. (Ref. 3) The adaptation technique can be described in the generalized coordinates as

$$\xi = \frac{\alpha \int_0^x q\,d\bar{x} + \beta \int_0^x k\,d\bar{x} - (\alpha + \beta - 1) \int_0^x q\,d\bar{x} \int_0^x k\,d\bar{x}}{\alpha \int_0^1 q\,dx + \beta \int_0^1 k\,dx - (\alpha + \beta - 1) \int_0^1 q\,dx \int_0^1 k\,dx} \tag{5}$$

where x - normalized arc length, q - flow parameter gradient, k - flow parameter curvature, α & β - weight factor assigned to gradients and curvatures. so that

$$\Delta\xi = \frac{[\,\alpha q + \beta k - (\alpha + \beta - 1) qk\,]\,\Delta x}{\alpha \int_0^1 q\,dx + \beta \int_0^1 k\,dx - (\alpha + \beta - 1) \int_0^1 q\,dx \int_0^1 k\,dx} \tag{6}$$

Then with R_1 defined as

$$R_1 = \frac{\alpha \int_0^1 q\,dx}{\alpha \int_0^1 q\,dx + \beta \int_0^1 k\,dx - (\alpha + \beta - 1) \int_0^1 q\,dx \int_0^1 k\,dx} \tag{7}$$

we have the maximum percentage change in the solution over a grid interval,

$$r = \frac{q\Delta x}{\int_0^1 q\,dx} = \frac{\Delta\xi}{R_1} - \frac{[(1-q)\beta \int_0^1 k\,dx + (1-\alpha) q \int_0^1 k\,dx]\Delta x}{\alpha \int_0^1 q\,dx}$$

$$\leq \frac{\Delta\xi}{R_1} = \frac{1}{NR_1} \tag{8}$$

since $\Delta\xi = 1/N$ and N+1 is the number of points on the coordinate line. If we take an equality in Eq. (8) with R_1 from Eq. (7) , we have

$$r = \frac{1}{NR_1}$$

$$= \frac{\alpha(1 - \int_0^1 k\,dx) \int_0^1 q\,dx + \int_0^1 q\,dx \int_0^1 k\,dx + \beta(1 - \int_0^1 q\,dx) \int_0^1 k\,dx}{N\alpha \int_0^1 q\,dx} \tag{9}$$

Ignoring the effect of the β term:

$$r = \frac{(1 - \int_0^1 k\,dx)\alpha \int_0^1 q\,dx + \int_0^1 q\,dx \int_0^1 k\,dx}{N\alpha \int_0^1 q\,dx} \tag{10}$$

$$\Rightarrow \alpha = \frac{\int_0^1 q dx \int_0^1 k dx}{\int_0^1 q dx \left(rN - 1 + \int_0^1 k dx \right)} \tag{11}$$

Similarly with R_2 defined as

$$R_2 = \frac{\beta \int_0^1 k dx}{\alpha \int_0^1 q dx + \beta \int_0^1 k dx - (\alpha + \beta - 1) \int_0^1 q dx \int_0^1 k dx} \tag{12}$$

we can get

$$\beta = \frac{R_2 \int_0^1 q dx \left[\alpha(1 - \int_0^1 k dx) + \int_0^1 k dx \right]}{\int_0^1 k dx \left(1 - R_2 + R_2 \int_0^1 q dx \right)} \tag{13}$$

With Boolean sum operation, we found that the choice of $R_1 = 1$ and $R_2 = 1$ still results in a very good adaptive grid.

GENERATE REDISTRIBUTED ALGEBRAIC GRID

All of the adaptive grids displayed in this paper are generated by the Non-Uniform Rational B-spline in surface (NURBS) or reparametrized uniform B-spline surface. The reparametrized uniform B-spline curve is applied to move the boundary points in order to keep the sharp corners (Fig.3). In general, the degree m NURBS surface (3-D) is defined as the projection of a tensor product B-spline in 4-D (Ref. 5-6):

$$\underset{\sim}{r}(\xi,\eta) = \frac{\sum_{i=0}^{NI} \sum_{j=0}^{NJ} B_{ij}^{m}(\xi,\eta) H_{ij} Q_{ij}}{\sum_{i=0}^{NI} \sum_{j=0}^{NJ} B_{ij}^{m}(\xi,\eta) H_{ij}} \tag{14}$$

where B_{ij}^{m} are the mth order bivariate B-spline basis functions. H_{ij} and Q_{ij} are the associated latice of weights and control points. In the grid redistribution process, a matrix form of bi-cubic NURBS was applied which can be formulated as (Ref. 7):

$$\underset{\sim}{r}(\xi,\eta) = [1 \ \xi \ \xi^2 \ \xi^3] M_{bl}^{3} [HQ] [M_{bl}^{3}]^T [1 \ \eta \ \eta^2 \ \eta^3]^T \tag{15}$$

$$\xi = \frac{t - t_i}{t_{i+1} - t_i} \quad , \quad \eta = \frac{s - s_i}{s_{i+1} - s_i} \tag{16}$$

where control points and weights [H Q] are as follow:

$$[HQ] = \begin{bmatrix} (HQ)_{i-1,j-1} & (HQ)_{i-1,j} & (HQ)_{i-1,j+1} & (HQ)_{i-1,j+2} \\ (HQ)_{i,j-1} & (HQ)_{i,j} & (HQ)_{i,j+1} & (HQ)_{i,j+2} \\ (HQ)_{i+1,j-1} & (HQ)_{i+1,j} & (HQ)_{i+1,j+1} & (HQ)_{i+1,j+2} \\ (HQ)_{i+2,j-1} & (HQ)_{i+2,j} & (HQ)_{i+2,j+1} & (HQ)_{i+2,j+2} \end{bmatrix} \tag{17}$$

The matrix M_{bl}^{3} is defined as

$$M_{bl}^{3} = \begin{bmatrix} b_{11} & b_{12} & b_{13} & b_{14} \\ b_{21} & b_{22} & b_{23} & b_{24} \\ b_{31} & b_{32} & b_{33} & b_{34} \\ b_{41} & b_{42} & b_{43} & b_{44} \end{bmatrix} \tag{18}$$

$$b_{11} = \frac{(t - t_{i+1})^2}{(t_{i+1} - t_{i-2})(t_{i+1} - t_{i-1})}, \quad b_{12} = 1 - (b_{11} + b_{13})$$

$$b_{21} = -3b_{11}, \quad b_{22} = -(b_{21} + b_{23})$$

$$b_{31} = 3b_{11}, \quad b_{32} = -(b_{31} + b_{33})$$

$$b_{41} = -b_{11}, \quad b_{42} = -(b_{41} + b_{43} + b_{44})$$

$$b_{13} = \frac{(t_{i-1} - t_i)^2}{(t_{i-1} - t_{i+2})(t_{i-1} - t_{i+1})}, \quad b_{14} = 0$$

$$b_{23} = \frac{3(t_{i+1} - t_i)(t_i - t_{i-1})}{(t_{i-1} - t_{i+2})(t_{i-1} - t_{i+1})}, \quad b_{24} = 0$$

$$b_{33} = \frac{3(t_{i+1} - t_i)^2}{(t_{i-1} - t_{i+2})(t_{i-1} - t_{i+1})}, \quad b_{34} = 0$$

$$b_{44} = \frac{(t_{i+1} - t_i)^2}{(t_i - t_{i+3})(t_i - t_{i+2})}$$

$$b_{43} = -(t_{i+1} - t_i)^2 \left[\frac{1}{(t_{i-1} - t_{i+1})(t_{i-1} - t_{i+2})} + \frac{1}{(t_i - t_{i+2})(t_i - t_{i+3})} + \frac{1}{(t_{i+2} - t_{i-1})(t_{i+2} - t_i)}\right]$$

The redistributed algebraic grid is generated by utilizing distribution mesh as parameter space. The convex hull, local support, and variation diminishing properties (Ref. 7) of B-spline functions contribute to the generation of the well-distributed smooth grid. The application of inverse NURBS formulation (Ref. 6) allows reevaluation of control points which influences the fidelity of surface geometry during the redistribution process. The redistributed grid is evaluated for positive areas and smoothness. If there is any negative area, the further more grid adaptation will not be executed.

APPLICATIONS

The initial grids were generated by (GENIE-2D-3D) (Ref. 1). The basic flow simulation codes is the computer code PARC2D (Ref. 10) which are algorithmically based on the Beam-Warming implicit finite difference scheme using approximate factorization. The routines for grid adaptation are incorporated in the PARC2D system with proper data flow.

(1) Wedge Problem with a 5 Degree Incline Angle at the Leading Edge. Using the theory developed for supersonic flow, it is possible to compute the exact behavior of the shock waves generated by single and double wedge in supersonic flow. In the wedge problem, the Mach number is 1.9, and the Reynolds number is 1.0×10^{10} with a grid size at 80 x 60. There is one shock and one reflected shock in the control volume. Without grid adaptation, the shock and the reflected shock are as thick as two small tapes. Even with a significant number of iterations (e.g. 10000 iterations)(Fig. 4). of the flow solver, the solution shows very little improvement. After grid adaptation, the two shocks appear thinner. Extremely thin shocks can be achieved by increasing grid adaptation numbers (Fig. 5). The grid adaptation was performed at every 300 iterations. The redistributed grids and their influence on the solution are presented in Figure 5. It can be seen that at every adaptation stage the pressure contours have indicated a crisper shock. A closer look at the changing grid behavior near the shock region is presented in Figure 6-7. In spite of extremely skewed grid lines, the code was able to execute and provide a better solution.

(2) Double Wedge Case with Grid Size 103 x 27 and 2.0 Mach Number. As expected, the shocks are thinner with grid adaptations, and the outlet near the mixture area of the second shock and the third shock is more clear (Fig. 8).

(3) Cylinder Case with Grid Size 80 x 100, Mach Number 3.0,and Zero Angle of Attack. The bow shock in front of the cylinder is captured better in the case of the adapted grid as shown in figure 9-10. Although the bow shock is a curve, the adaptive grid also bends along the shock wave.

It is generally well known that either rapidly varying the step size or the skew grid angle can lead to poor accuracy when using finite difference approximations. Dwyer has shown by numerical experiments that variable grids coupled with adaptive techniques are accurate. (Ref. 9) In this paper we also observed in several cases that high skew angle grids coupled with adaptive techniques can excellently resolve the shock (Fig. 5-10). We also acknowledge that if the orientation of the grid line is aligned with the shock wave, the shock wave is captured exactly (Fig. 11). Thus, not only the cluster of the grid points near the shock is necessary but also the alignment of the grid points with the shock wave is important. We found that during the adaptation, the alignment of the grid points with shock wave will be accomplished by forming the skewed grid lines, according to the flow solutions. It is hoped that mathematical analysis could be developed to prove this observation, but the present investigators have not proceeded in this pursuit. We hope it will be accomplished in the near future.

(4) Airfoil NACA 0012 with Grid Size is 180 x 160, Mach Number 0.799, and the Angle of Attack 1.25. The upper surface shock is thinner with the grid adaptation. The lower surface has no weak shock if no grid adaptation is applied, but with grid adaptation, the weak shock was captured (Fig. 12). Comparing the C_p vs x/c charts, it is clear that the adaptive grid caught both shocks much better than the initial grid did (Fig. 13), but the adaptive grid loses the grid concentration at the leading edge and the tail. This is because the control field is so large that the effect of concentrating grid lines near the high gradient and/or the high curvature is spread to the whole field. The strategies that can improve this kind of condition are modifying the weight function by controlling the distribution near the body surface or subdividing the whole field into several blocks with some smaller blocks near

the surfaces of the airfoil and applying the local grid adaptation. The second strategy needs the development of a multi-block adaptive grid system. Both strategies are currently under investigation.

CONCLUSION

With a new weight function formula, a new method that applies the NURBS surface in the algebraic adaptive grid generation system is introduced. The effect of this new adaptive grid system is pretty good in capturing the shock wave for some smaller control field. The grid adaptation strategies that are applied to catch the high gradient and/or high curvature area are used not only to cluster grid points near those areas but also to move the grid points to align along the high solution derivative areas. For complicated control fields, the multi-blocks adaptive grid system may be required. The weight function that is suitable for laminar or turbulance flow simulation which need very small cells near body surface, also needs to be investigated. The extension of this 2-D general adaptive grid system to a three dimensional problem and its adaptation to a multiblock environment is currently underway.

References

1. Soni, B. K., "GENIE: GENeration of Computational Geometry-Grids for Internal Flow Configurations", *proceedings of Numerical Grid Generation in Computational Fluid Mechanics '88*, Miami, FL, 1988.
2. Soni, B. K., "Grid Generation for Internal Flow Configurations", *Journal of Computers and Mathematics with Applications, 1991.*
3. Thompson, J. F., "A Survey of Dynamically-Adaptive Grids in The Numerical Solution of Partial Differential Equations", *Applied Numerical Mathematics 1*, p. 3, North-Holland, 1985.
4. Connett, W. C., Agarwal, R. K., and Schwartz, A. L., "An Adaptive Grid-Generation Scheme for Flow Field Calculations", AIAA-87-0199.
5. Abolhassani, J. S., Smith, R. E., and Surendra, N. T., "Grid Adaptation for Hypersonic Flow", AIAA-87-1169.
6. Yamaguchi, F., "Curves and Surfaces in Computer Aided Geometric Design", Springer-Verlag, 1988.
7. Yoon, Y.-H., "Enhancements and Extensions of EAGLE Grid Generation System", Ph. D. Dissertation, Mississippi State University, Mississippi, MS,1991.
8. Thompson, J. F., Warsi, Z. U. A., Mastin, C. W., Adaptive Grids, in: *Numerical Grid Generation Foundations and Applications* (North-Holland, 1985), p. 370-378.
9. Dwyer, H. A., "Grid Adaption for Problem in Fluid Dynamics", AIAA Journal Vol. 22. No. 12, December 1984.
10. Cooper, G. K., Sirbough, J. R., "PARC Code: Theory and Usage", AEDC-TR-89-15, Arnold Engineering Development Center, Arnold AFB.

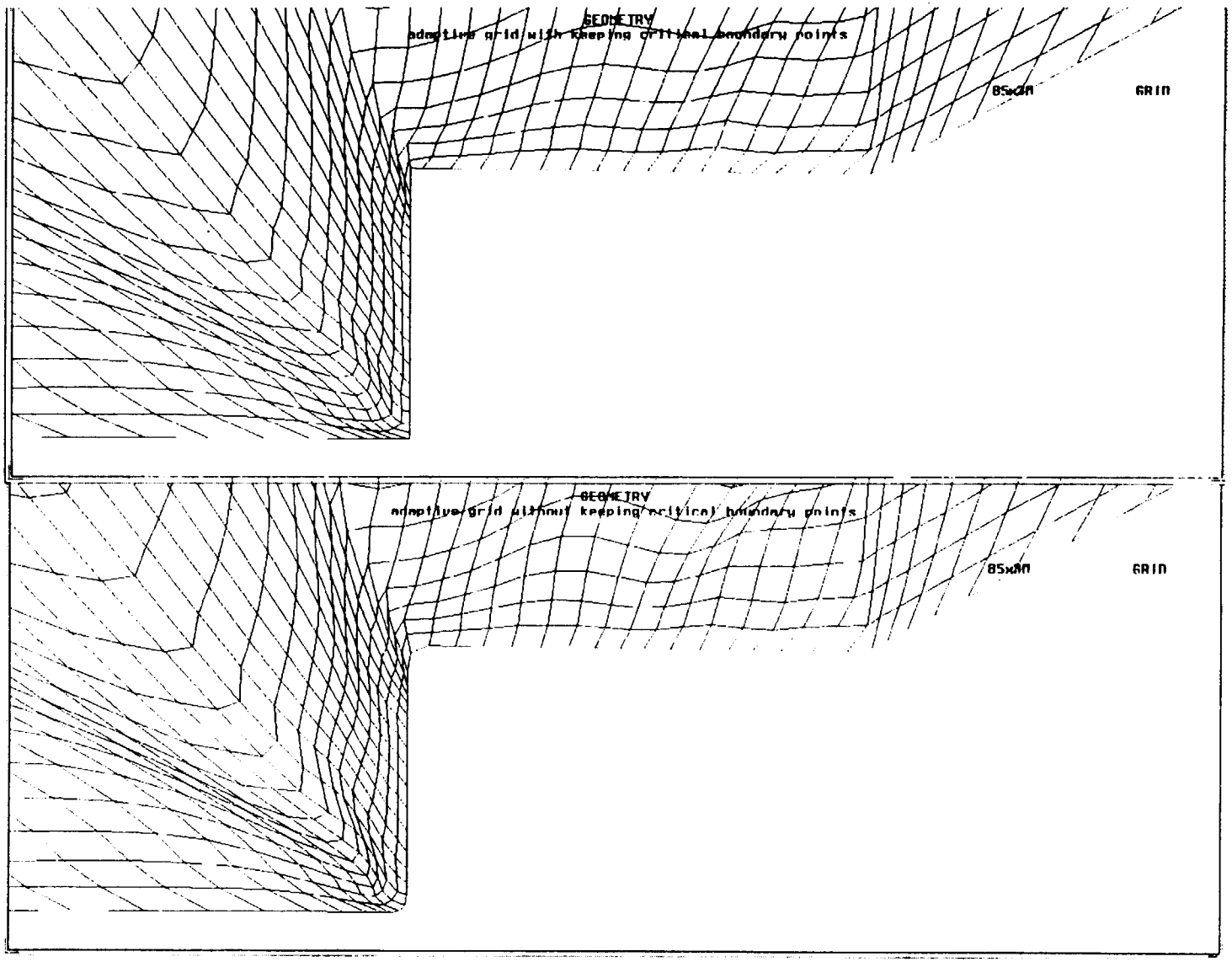

Figure 3.
Use B-Spline curve to keep sharp corners.

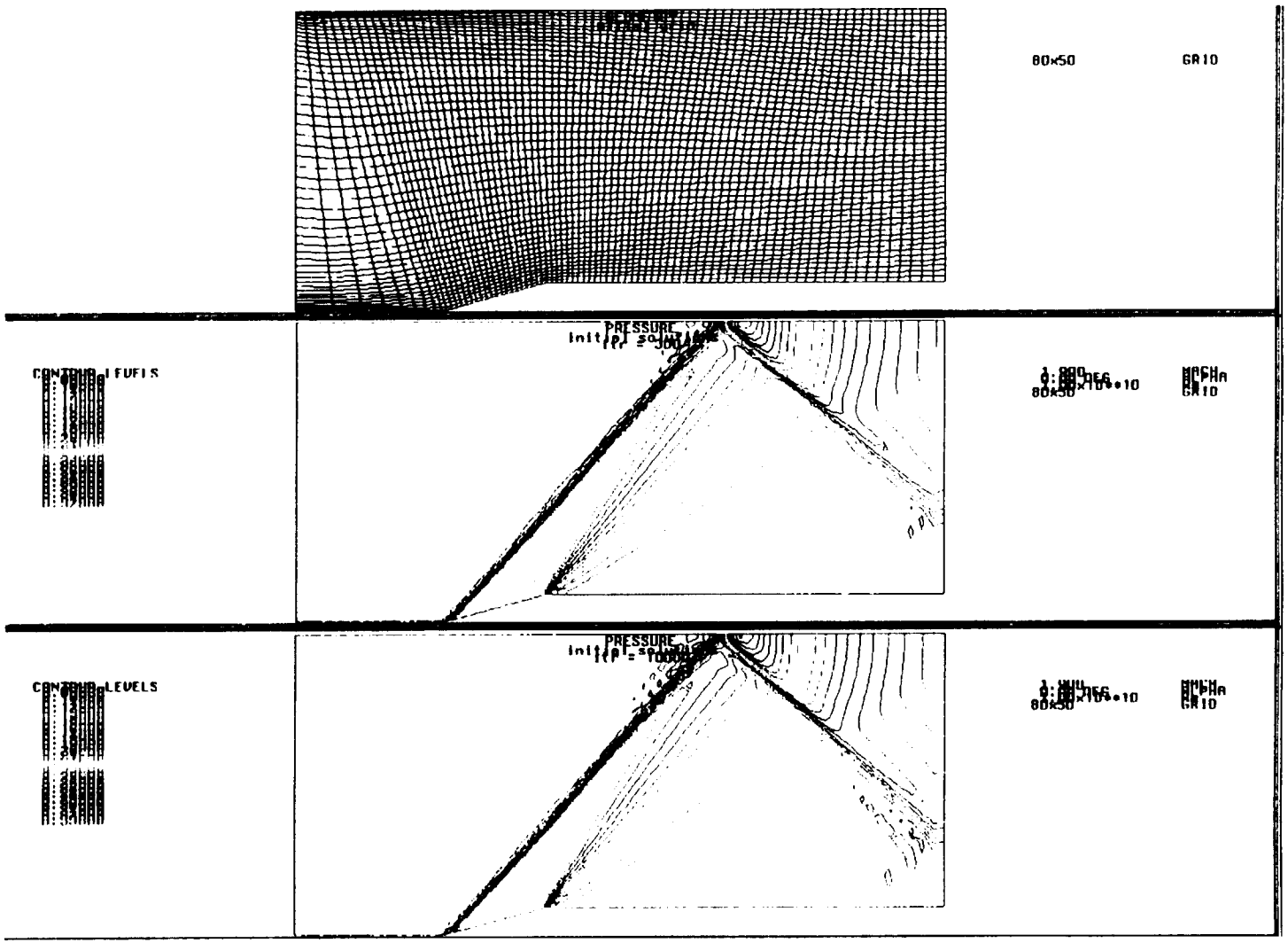

Figure 4.
Single wedge initial grids & solutions after 300 & 10000 iterations.

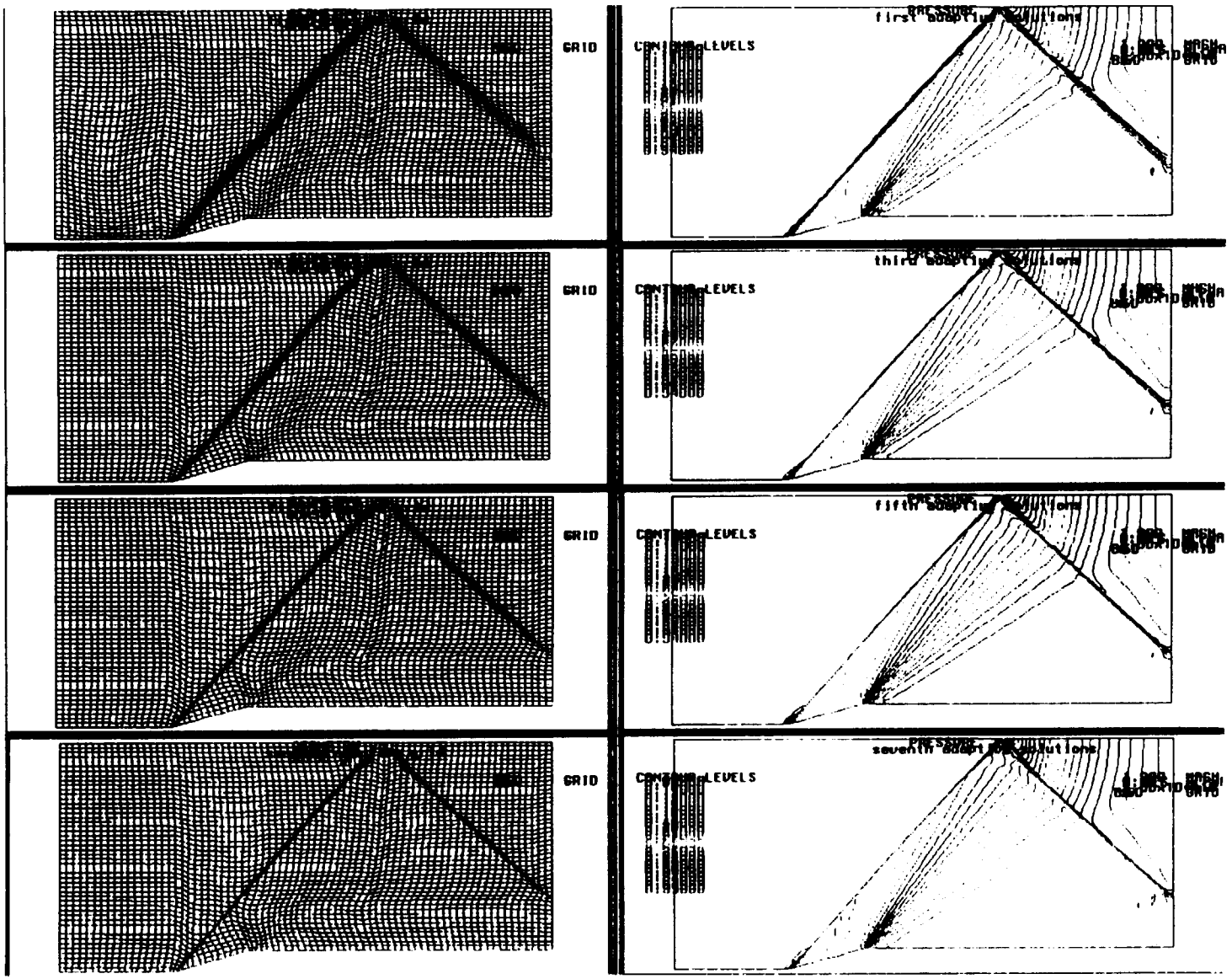

Grids

Pressure contours

Figure 5.
Single wedge grid adaptation process.

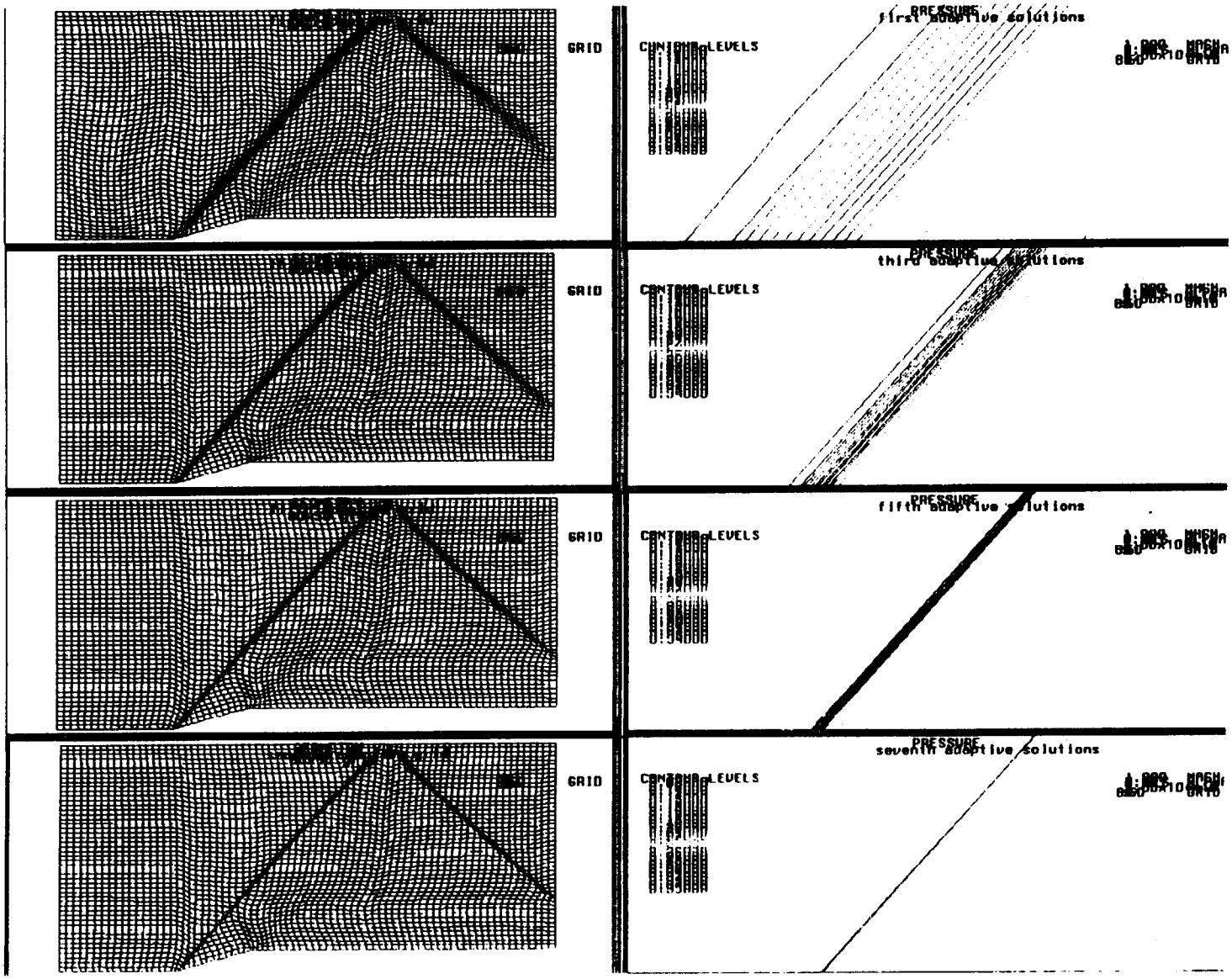

Figure 6.
Single wedge, closer pressure contour look near shock region.

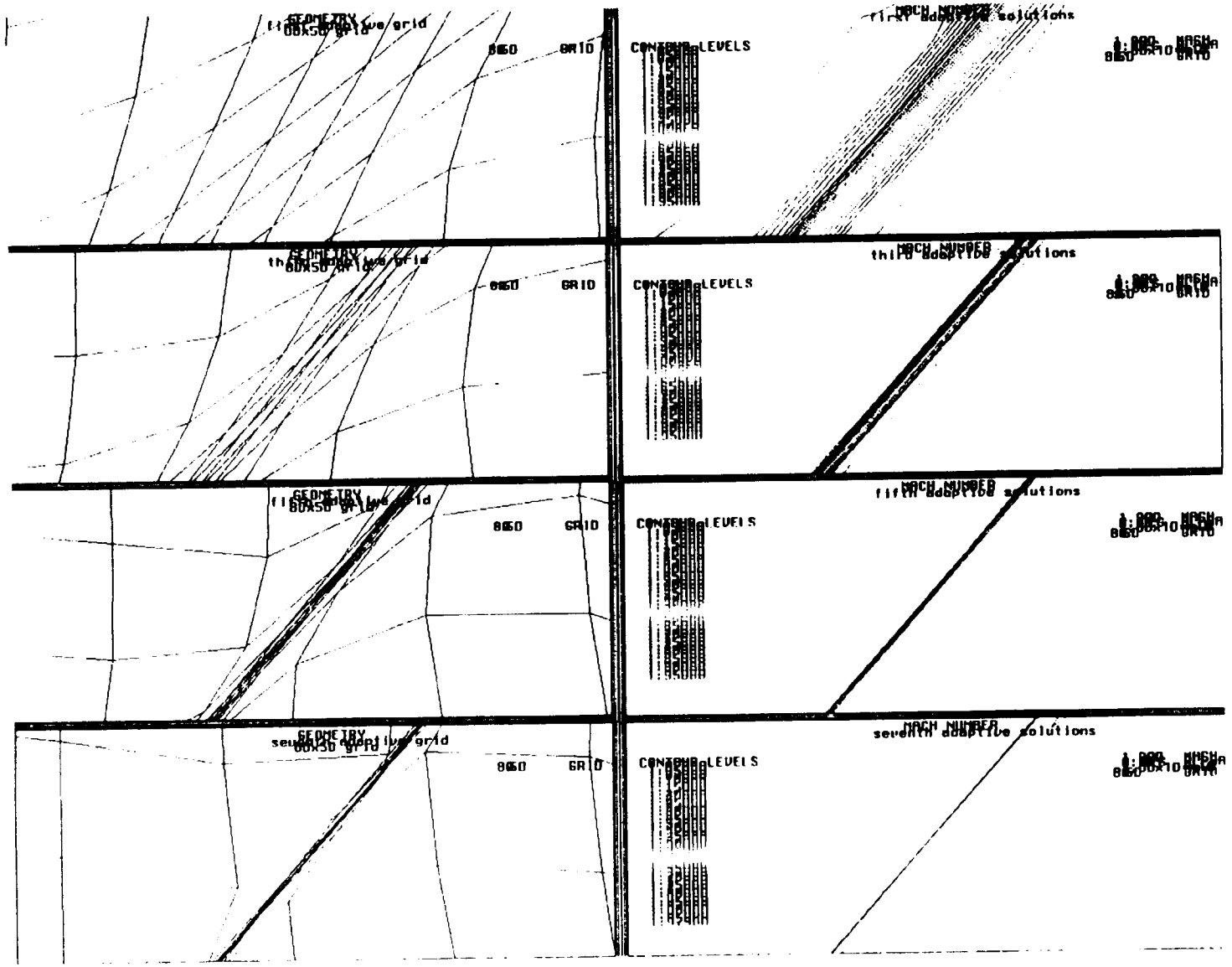

Figure 7.
Single wedge, closer Mach number contour look near shock region.

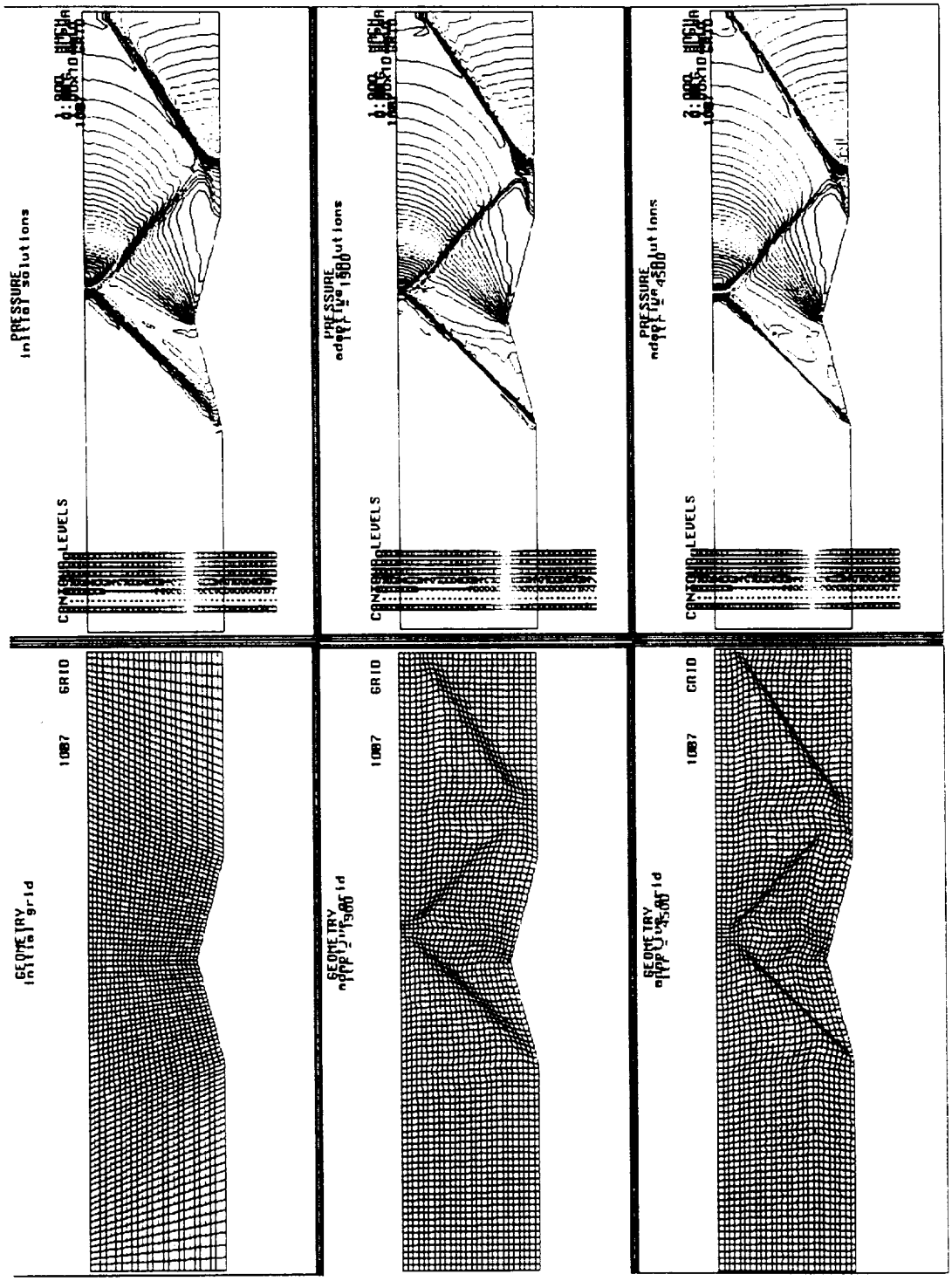

Figure 8.
Double wedge case non-adaptive/adaptive simulation.

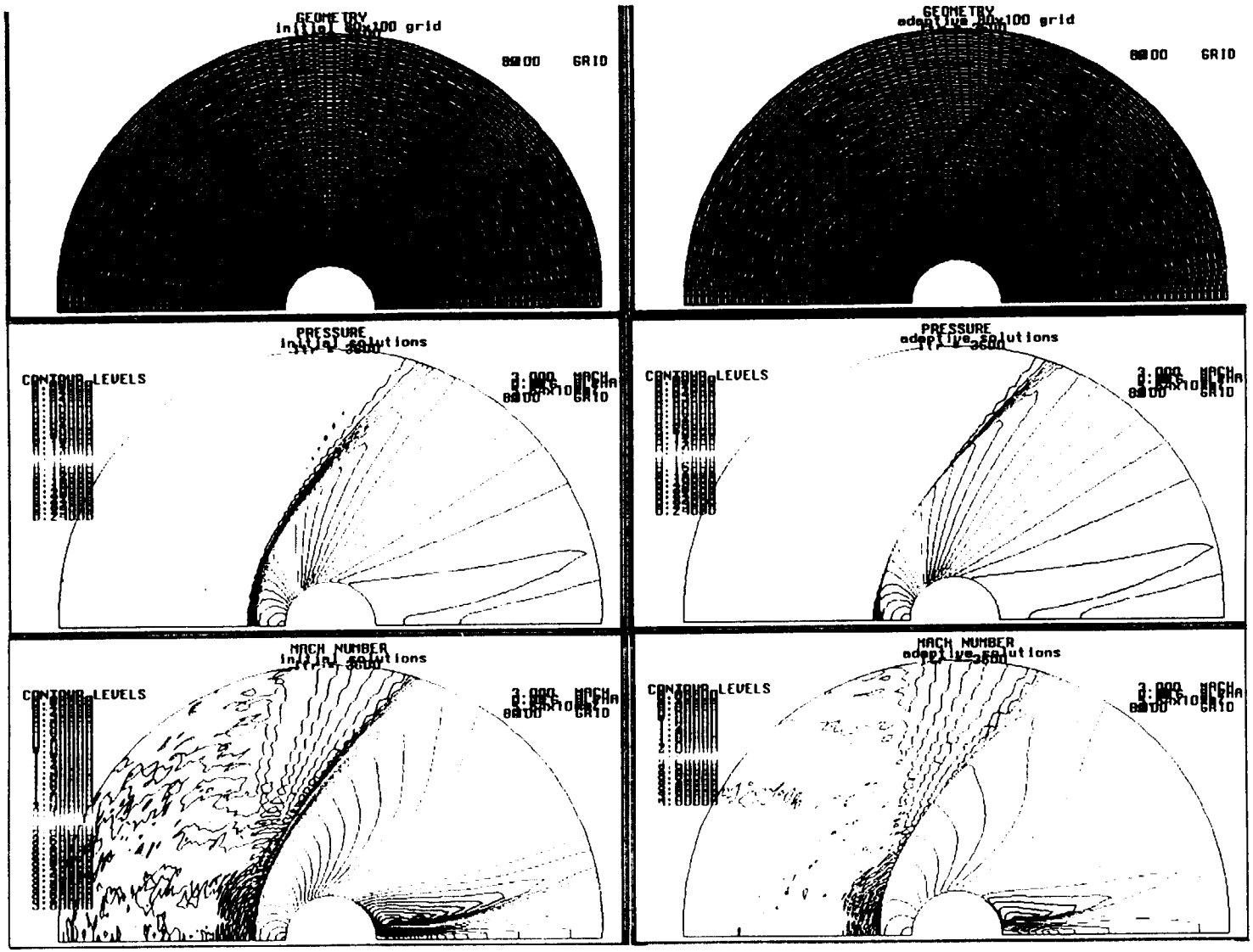

Initial grid simulation

Adaptive grid simulation

Figure 9.
Flow around cylinder initial/adaptive cases.

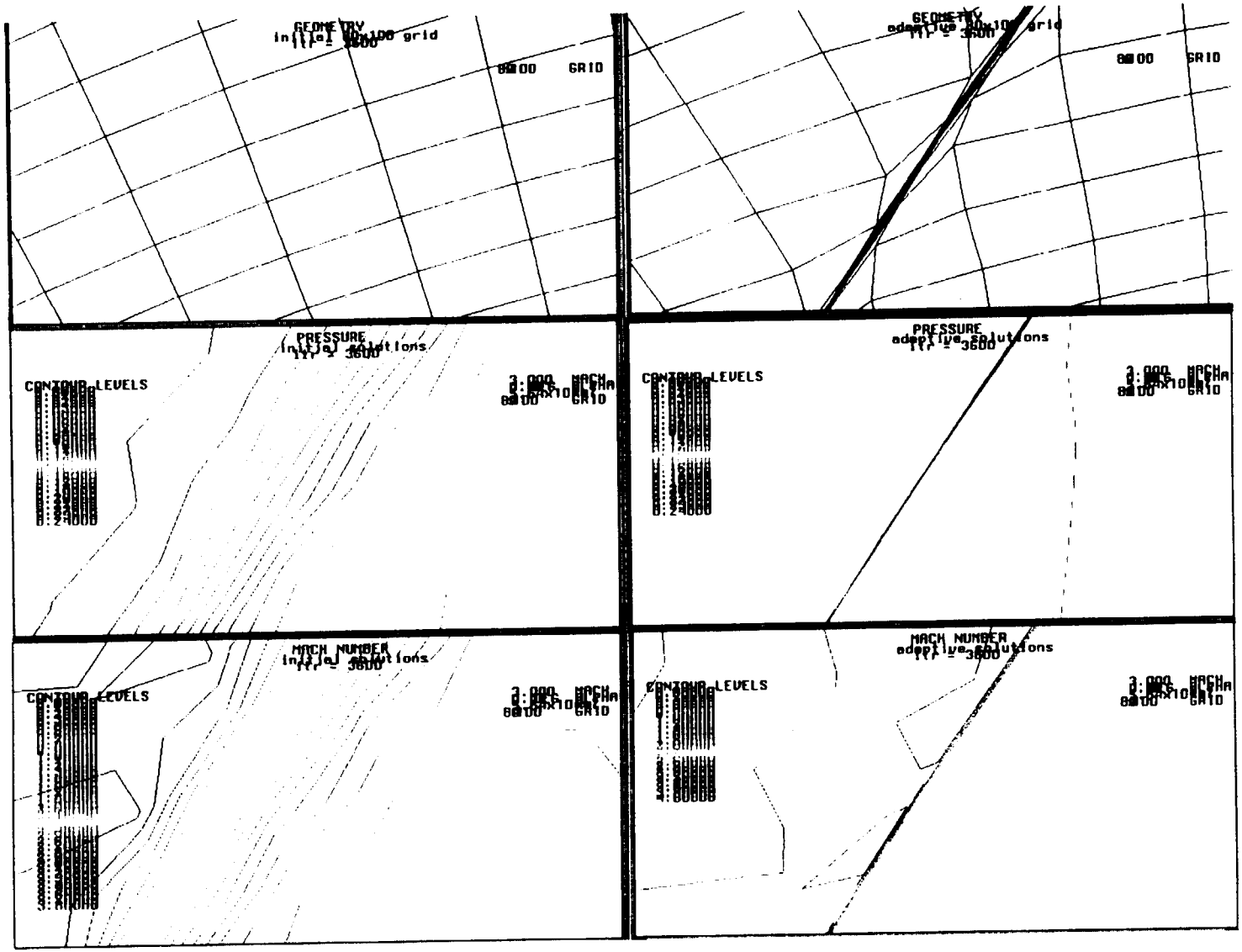

Figure 10.
Flow around cylinder, closer look near shock region.

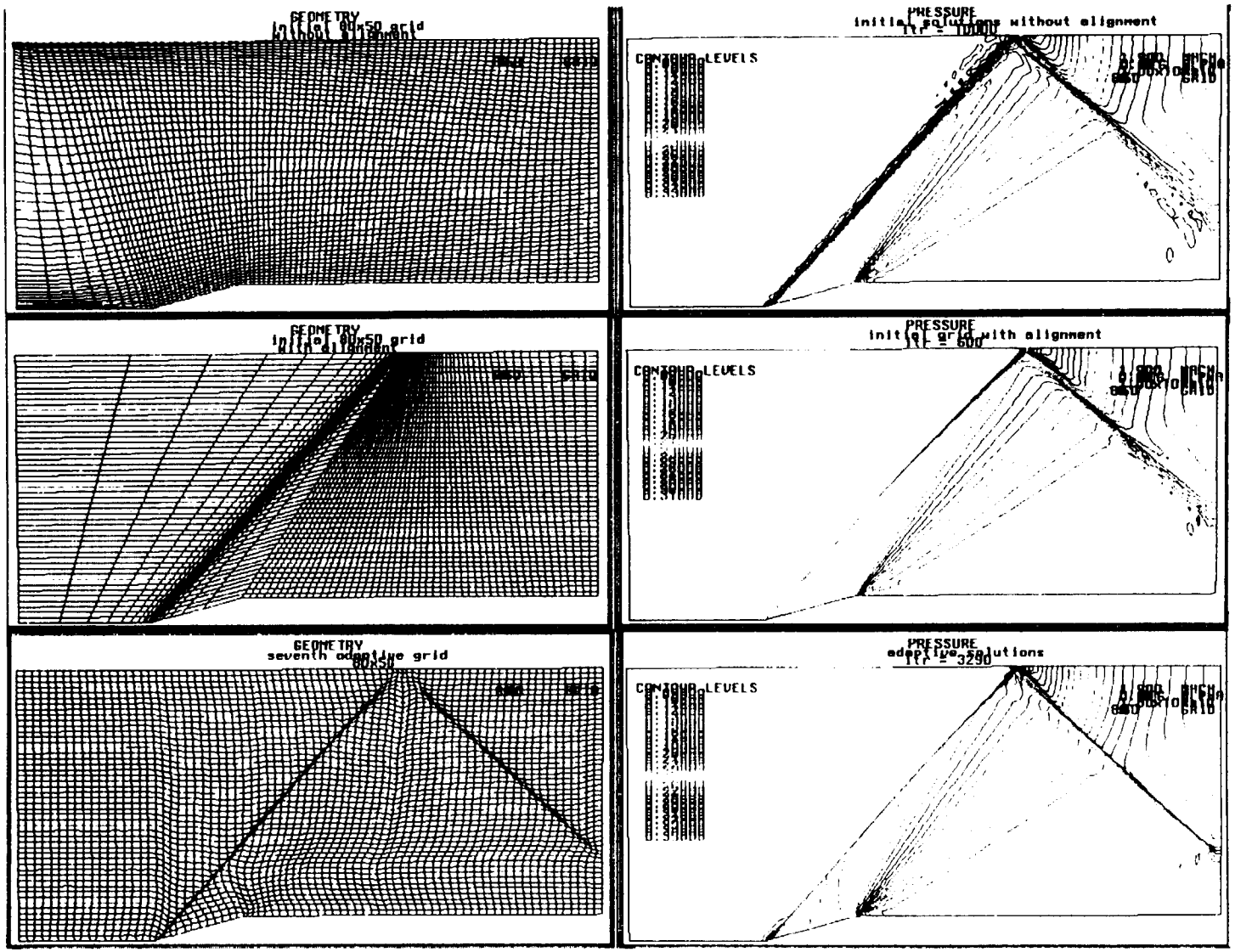

Figure 11.
Grid lines align with the shock wave capture shock exactly.

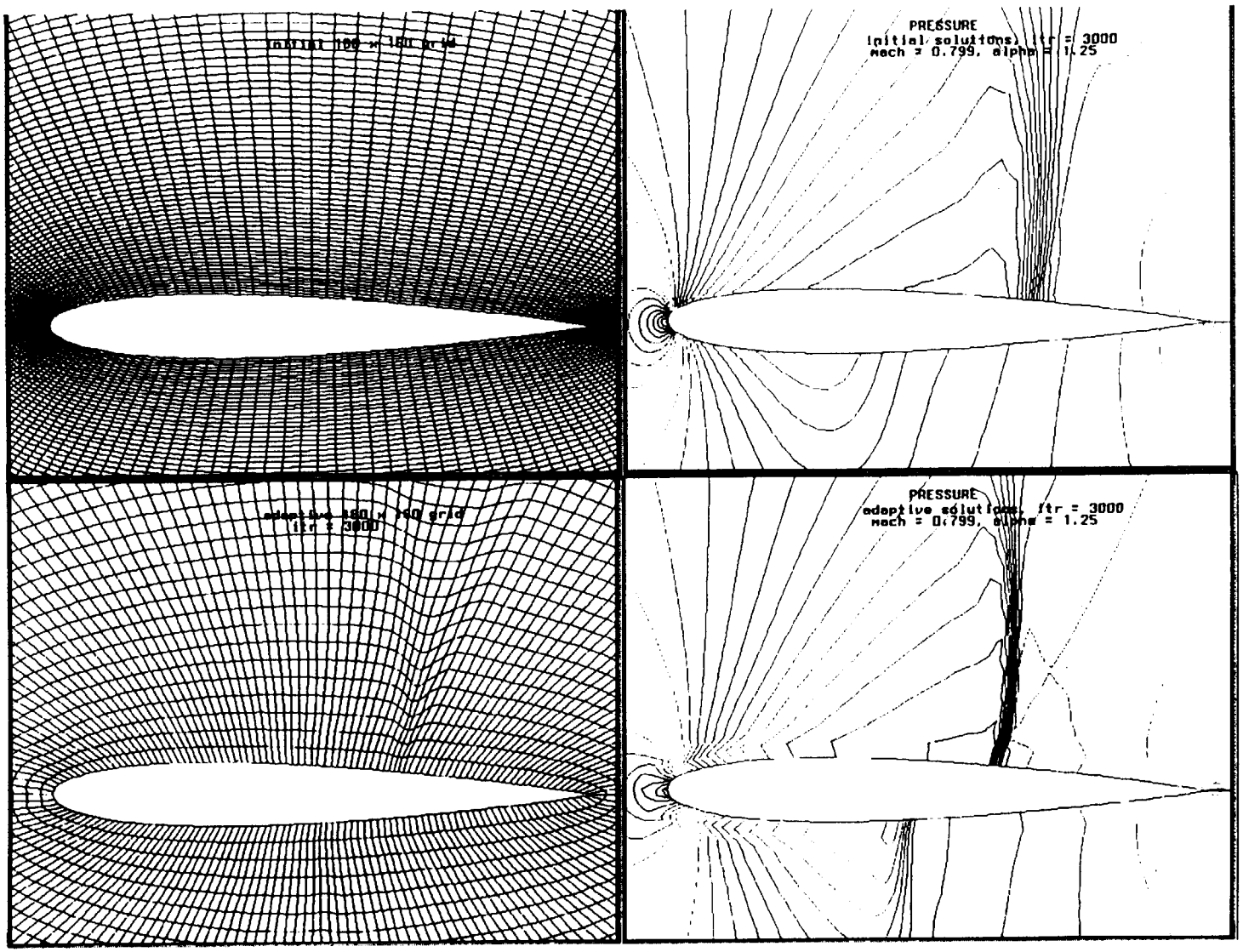

Figure 12.
Airfoil NACA0012 case non-adaptive/adaptive grid/solution.

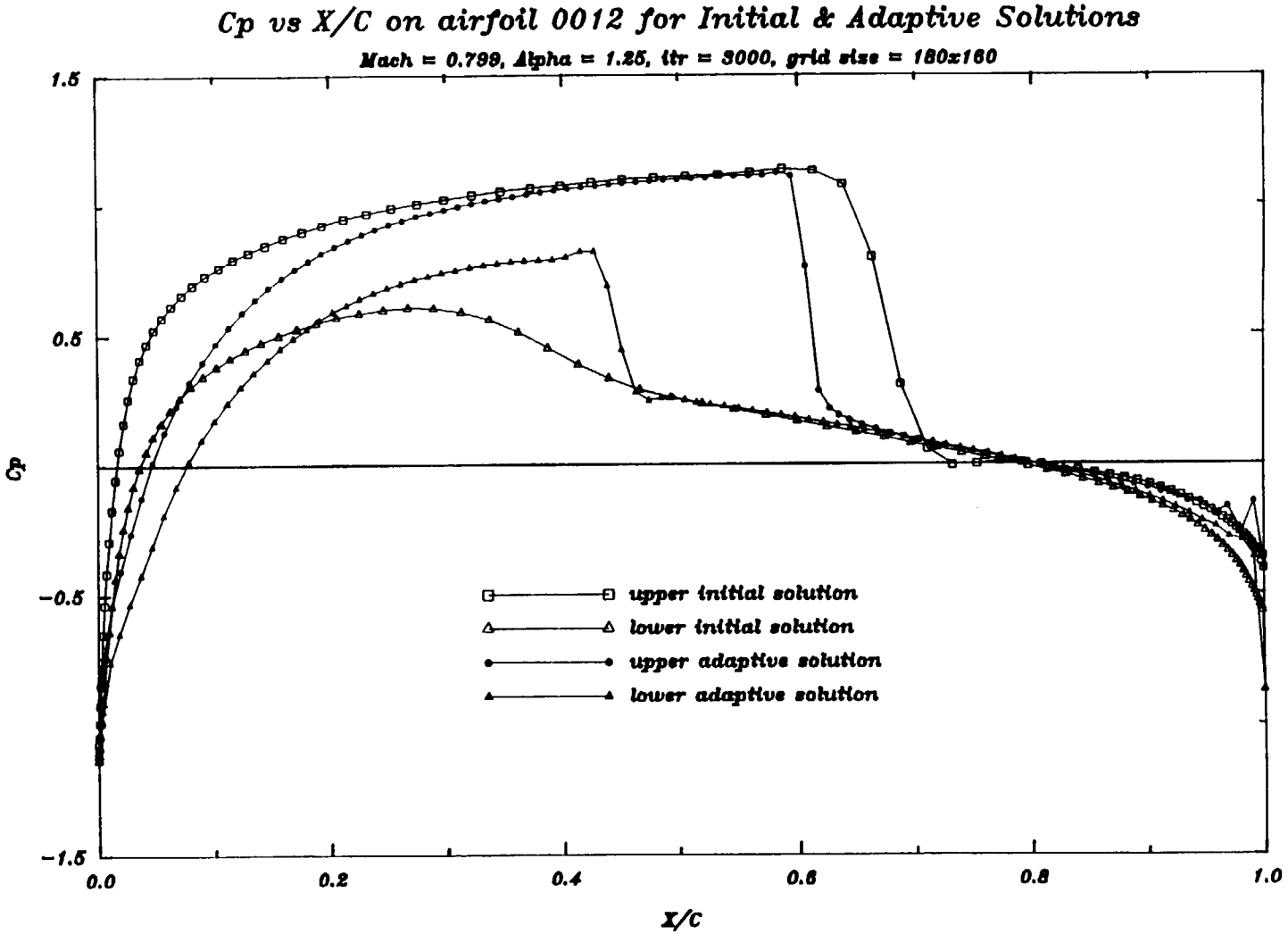

Figure 13.
Airfoil NACA0012 case Cp vs x/c plot.